European Journal of Medicinal Chemistry 45 (2010) 727–737

Contents lists available at ScienceDirect

European Journal of Medicinal Chemistry

journal homepage: http://www.elsevier.com/locate/ejmech

Original article

Radiosynthesis and radiopharmacological evaluation of cyclin-dependent kinase 4 (Cdk4) inhibitors

Lena Koehler [a], Franziska Graf [a], Ralf Bergmann [a], Jörg Steinbach [a], Jens Pietzsch [a], Frank Wuest [a,b,*]

[a] Institute of Radiopharmacy, Research Center Dresden-Rossendorf, Dresden, Germany
[b] Department of Oncology, University of Alberta, 11560 University Ave, Edmonton, Canada

ARTICLE INFO

Article history:
Received 5 August 2009
Received in revised form
30 October 2009
Accepted 12 November 2009
Available online 24 November 2009

Keywords:
Iodine-124
Cell cycle
Cyclin-dependent kinase 4 inhibitor
Positron emission tomography (PET)

ABSTRACT

Tumor cells are characterized by their loss of growth control resulting from alterations in regulating pathways of the cell cycle, such as a deregulated cyclin-dependent kinase (Cdk) activity and/or Cdk expression. Appropriately radiolabeled Cdk4 inhibitors are discussed as promising molecular probes for imaging cell proliferation processes and tumor visualization by PET. This work describes the design, synthesis and radiopharmacological evaluation of two ^{124}I-labeled Cdk4 inhibitors as potential radiotracers for imaging of Cdk4 *in vivo*. Treatment of a solution containing labeling precursors with [^{124}I]NaI gave radiolabeled Cdk4 inhibitors **[^{124}I]CKIA** and **[^{124}I]CKIB** in radiochemical yields of up to 35%. ^{124}I-labeled radiotracers **[^{124}I]CKIA** and **[^{124}I]CKIB** were used in cell uptake studies as well as biodistribution studies in Wistar rats and small-animal PET in tumor-bearing mice. *In vitro* radiotracer uptake studies in adherent tumor cells using **[^{124}I]CKIA** showed substantial uptake in HT-29 and FaDu cells (750–850 %ID/mg protein **[^{124}I]CKIA** and 900–1000 %ID/mg protein **[^{124}I]CKIB**) after 1 h at 37 °C. Biodistribution of **[^{124}I]CKIA** and **[^{124}I]CKIB** showed rapid blood clearance of radioactivity and an accumulation as well as metabolization in the liver. Both radiotracers were administered intravenously to mouse FaDu xenograft tumor model and imaging studies were performed on a small-animal PET scanner. Both imaging techniques showed only little uptake of both radiotracers in the FaDu tumor xenografts.

1. Introduction

Tumorigenesis is a result of cell-cycle dysregulation leading to an uncontrolled cellular proliferation [1–4]. An aberrant cell proliferation is a hallmark of cancer. In healthy tissue, cell division occurs in the context of a highly regulated concert of molecular events known as the cell cycle. The cell cycle is divided into four distinct phases: DNA synthesis (S phase), mitosis (M phase), and the gaps of varying length between these periods called G_1 and G_2. Non-dividing cells remain in a resting or quiescence stage named G_0 before they re-enter into phase G_1.

The regulation of the cell cycle is governed and controlled by specific proteins, which are activated and deactivated mainly through phosphorylation/dephosphorylation processes in a precise timely matter. The key proteins that coordinate the initiation, progression, and completion of cell-cycle program are cyclin-dependent kinases (Cdks). Cyclin-dependent kinases belong to the serine–threonine protein kinase family. They are heterodimeric complexes composed of a catalytic kinase subunit and a regulatory cyclin subunit. Cdk activity is controlled by association with their corresponding regulatory subunits (cyclins) and Cdk inhibitor proteins (Cip & Kip proteins, INK4s), by their phosphorylation state, and by ubiquitin-mediated proteolytic degradation [5–8]. In early to mid G_1 phase, when the cell is responsive to mitogenic stimuli, activation of Cdk4-cyclin *D* and Cdk6-cyclin *D* induces phosphorylation of the retinoblastoma protein (pRb). Phosphorylation of pRb releases the transcription factor E2F, which enters the nucleus to activate transcription of other cyclins which promote further progression of the cell cycle [9,10]. Cdk4 and Cdk6 are closely related proteins with basically indistinguishable biochemical properties [11]. Genetic analysis of numerous human cancers has shown that in more than 80% of human neoplasia the cyclin D-Cdk4/INK4/pRb/E2F pathway has been altered, making Cdk4 an attractive target for the development of anti-cancer drugs [12,13].

Over the last years, considerable effort has been made to screen and design small molecule Cdk inhibitors [14]. Several drug discovery programs have identified potent small molecule Cdk inhibitors from a variety of chemical classes, which include purine analogues, pyrimidine analogues, indenopyrazoles, pyridopyrimidines, pyrozolopyridines, indolocarbazoles, pyrrolocarbazoles,

* Corresponding author. Tel.: +1 780 989 8150; fax: +1 780 432 8483.
E-mail address: frankwue@cancerboard.ab.ca (F. Wuest).

0223-5234/$ – see front matter © 2009 Elsevier Masson SAS. All rights reserved.
doi:10.1016/j.ejmech.2009.11.020

oxindoles, and aminothiazoles [14]. Although much biochemical evidence supports targeting Cdk4 as the most important Cdk for regulating cell proliferation, most drug development programs have produced compounds which inhibit multiple Cdks, with Cdk2 and Cdk1 being particularly common targets [15,16]. Several of the compounds are currently in preclinical and clinical trials including flavopiridol [17–19], staurosporine UCN-01 [20,21], BMS-387032 [19], olomoucine [5,22,23], CYC202 [24,25], NU6102 [26], CR8 [27], AT7519 [28], and SCH-727965 [29–31] (Fig. 1).

However, evidence has been reported in the literature that mammalian cells can continue to proliferate in the absence of Cdk2 activity [32]. Hence, Cdk2 activity seems to be not essential for cell proliferation in various cancers. These results suggest that Cdk2 may not be the ideal target for inhibition by small molecules to treat cancer. The possible compensation of Cdk2 activity by Cdk4 and the upregulation of Cdk4 activity in many human cancers have shifted attention of cancer drug discovery towards Cdk4 as the more important cell-cycle Cdk target.

The design of selective Cdk4 inhibitors represents a formidable challenge due to the common folding pattern of numerous kinases and their kinase domains including the ATP binding pockets. Over the last years, various Cdk4 inhibitors have been described in the medicinal chemistry literature. The structure-based design of potent and selective Cdk4 inhibitors led to the development of several classes of compounds, including pyrido[2,3-*d*]pyrimidines, 2-anilinopyrimidines, diaryl ureas, benzoyl-2,4-diaminothiazoles, indolo[6,7-a]pyrrolo[3,4-c]carbazoles, and oxindoles [14]. Especially various compounds based on a pyrido[2,3-*d*]pyrimidine scaffold containing a side chain at the *C*2 position were shown to be highly potent Cdk4 inhibitors ($IC_{50} < 20$ nM) with favorable selectivity profile over Cdk1, Cdk2, and other kinases (Fig. 2) [33,34]. Compound PD 0332991 has entered clinical trial for cancer therapy [35].

The iodine-containing pyrido[2,3-*d*]pyrimidine-7-one **CKIA** has been reported as a very potent (IC_{50} (Cdk4) = 5 nM) and selective Cdk4 inhibitor (IC_{50} (Cdk1 and Cdk2) >360 nM) [36]. Moreover, the

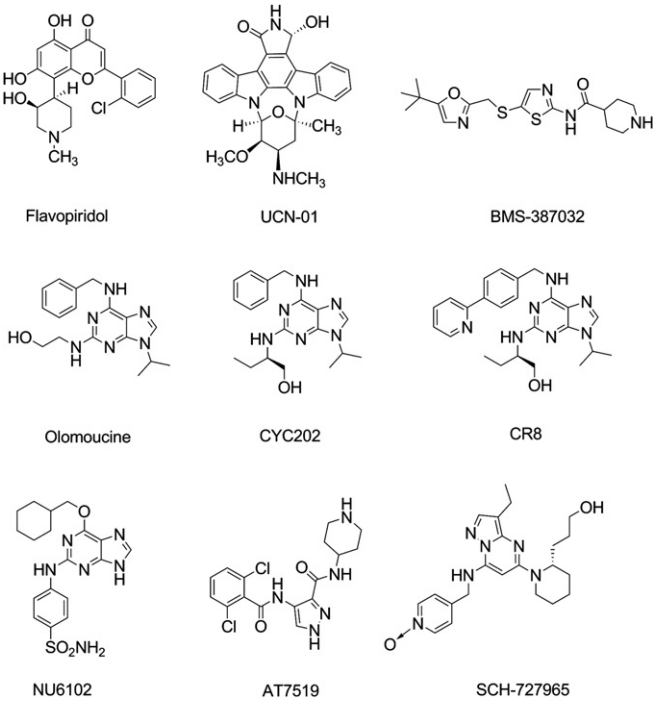

Fig. 1. Cdk inhibitors Flavopiridol, UCN-01, BMS-387032, olomoucine, CYC202, CR8, AT7519, SCH-727965, and NU6102.

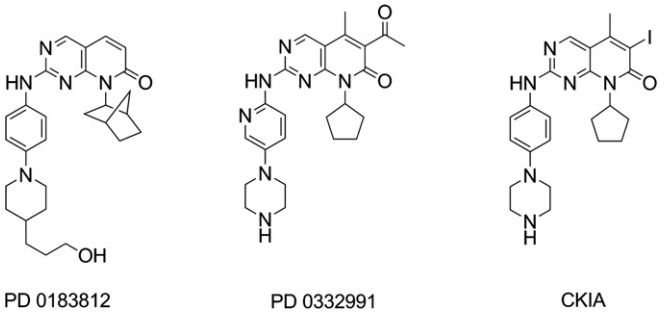

Fig. 2. Pyrido[2,3-*d*]pyrimidines containing a side chain at position *C*2 as potent and selective Cdk4 inhibitors [35,36,47].

iodine substituent in compound **CKIA** represents an attractive site for isotopic substitution with radioiodine isotopes to give the corresponding radiotracers for molecular imaging purposes. In previous work we showed that Cdk4 inhibitor **CKIA** and pyridine-containing analog **CKIB** act as tumor cell growth inhibitors via specific inhibition of the Cdk4/INK4/pRb/E2F signaling pathway and induction of G1 arrest in tumor cells [44].

Within the arsenal of molecular imaging methodologies, positron emission tomography (PET) is a particularly powerful technique to provide quantitative kinetic information of metabolic pathways and physiological processes *in vivo* [37].

The positron emitter iodine-124 (^{124}I) is an attractive radionuclide for the design, synthesis and radiopharmacological evaluation of iodine-containing compounds. Its convenient 4.18 d half-life allows extended synthesis protocols, and longitudinal imaging studies using small-animal PET [38,39]. The labeling technique for ^{124}I is well established, and this approach is continuously being used in the labeling and PET imaging of various biologically active compounds.

Currently, an exact and accurate assessment of functional Cdk4 expression in tumors or other tissues can only be achieved by laborious analyses of invasively acquired biopsies. Moreover, instability of Cdk4 mRNA and protein leads to further difficulties in terms of the intervals between tissue sampling and time of analysis. The development of a PET imaging probe for monitoring Cdk4 expression *in vivo* would provide data on functional Cdk4 protein expression in tumor development and progression. Moreover, the development and *in vivo* study of appropriately radiolabeled selective Cdk4 inhibitors would provide pharmacological data, which may help to further understand their exact physiological actions and metabolic pathways.

This work describes the design, synthesis and radiopharmacological evaluation of two ^{124}I-labeled Cdk4 inhibitors (8-cyclopentyl-6-[^{124}I]iodo-5-methyl-2-(4-piperazin-1-yl-phenyl-amino)-8*H*-pyrido[2,3-*d*]pyrimidin-7-one (**[^{124}I]CKIA**) and 8-cyclopentyl-6-[^{124}I]iodo-5-methyl-2-(5-(piperazin-1-yl)pyridin-2-ylamino)-8*H*-pyrido[2,3-*d*]pyrimidin-7-one (**[^{124}I]CKIB**)) as potential radiotracers for imaging Cdk4 expression *in vivo*. The radiopharmacological characterization of radiotracers **[^{124}I]CKIA** and **[^{124}I]CKIB** involved cellular uptake studies, metabolism and biodistribution studies in normal rats, and small-animal PET studies in NMRI nu/nu mice bearing the human head and neck squamous cell carcinoma tumor FaDu.

2. Results and discussion

2.1. Chemistry and radiosynthesis

The key step within the synthesis of pyrido[2,3-*d*]pyrimidine-based compounds as potent and selective Cdk4 inhibitors is the

introduction of amino-substituted side chains by displacement of the sulfoxide group at the *C*2 position of the pyrido[2,3-*d*]pyrimidine-7-one core [33,36]. The overall synthesis scheme for the preparation of reference compounds **CKIA** and **CKIB**, and labeling precursors **6** and **7** is depicted in Scheme 1.

Introduction of (4-aminophenyl)piperazine-containing side chain **2** into sulfoxide **1** to give compound **4** was accomplished in 75% yield at elevated temperature in DMSO, whereas application of DMSO as the solvent failed in the case of (2-amino-pyridin)piperazine-containing side chain **3** due to the formation of numerous side products during the reaction. Replacement of DMSO with toluene as the solvent gave the desired compound **5** in moderate chemical yield of 38%.

Removal of the Boc protecting group was easily achieved by the treatment of piperazines **4** and **5** with aqueous HCl at room temperature. Subsequent silica-gel purification gave the reference compounds **CKIA** and **CKIB** in excellent chemical yields of 95%.

Several radioiodination reactions involving organometallic intermediates have been shown to be very effective, rapid and site-specific methods for the incorporation of iodine isotopes into small molecules [40]. Especially the use of aromatic and vinylic organostannanes as labeling precursors gave very good results for radioiodinations via iodo-destannylation reactions. Thus, we prepared organostannanes **6** and **7** as precursors for radiolabeling with iodine-124. Organostannanes **6** and **7** were prepared via Pd-catalyzed cross coupling reaction between iodides **4** and **5**, and an excess of hexamethylditin (Sn_2Me_6) in 32% and 55% yield, respectively, after silica-gel chromatography.

Incorporation of ^{124}I into *C*-6 position of pyrido[2,3-*d*]pyrimidine compounds was accomplished under mild conditions through electrophilic substitution employing a regioselective iodo-destannylation reaction of *C*-6 trimethylstannyl-substituted compounds **6** and **7** with [^{124}I]NaI in the presence of a mild oxidizing agent (immobilized chloramine-T or Iodogen®). Subsequent removal of the Boc protecting group afforded the desired radiolabeled compounds. The general reaction scheme for the radiosynthesis of ^{124}I-labeled Cdk4 inhibitors **[^{124}I]CKIA** and **[^{124}I]CKIB** is given in Scheme 2.

For the optimization of the reaction conditions the influence of the amount of stannylated labeling precursor and the oxidizing agent on the radiochemical yield was tested. The optimization was performed with trimethylstannyl-precursor **6** and 2–3 MBq of [^{124}I]NaI (3–4 µl of [^{124}I]NaI in 0.25 M NaOH) at room temperature. The results are summarized in Table 1.

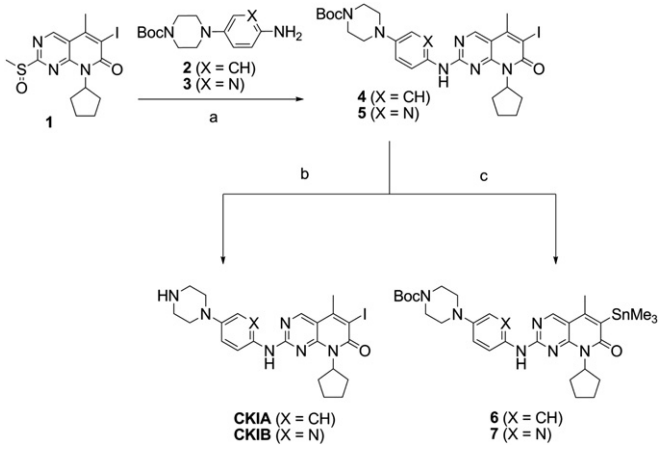

Scheme 1. Synthesis route for reference substances CKIA and CKIB, and labeling precursors **6** and **7**: (a) DMSO or toluene, 100 °C, 16 h; (b) dioxane, 6 M HCl, r.t., 2 h; (c) Sn_2Me_6, tetrakis(triphenyl-phosphine)palladium(0), dioxane, reflux, 8 h.

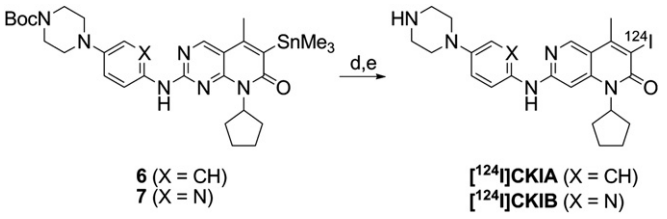

Scheme 2. Radiosynthesis of ^{124}I-labeled Cdk4 inhibitors **[^{124}I]CKIA** and **[^{124}I]CKIB**: (d) [^{124}I]NaI, DMSO, MeOH, HOAc, Iodogen®, r.t., 10 min; (e) TFA, 50 °C, 20 min.

Varying amounts of labeling precursor **6** were dissolved in a 1:3 mixture of DMSO and 5% acetic acid in methanol in an Eppendorf vial. The use of DMSO as a solvent was necessary since compound **6** showed only poor solubility in methanol containing 5% of acetic acid. Besides the beneficial effect of DMSO to ensure complete solubility, DMSO was also reported to improve the efficiency of radioiodination reactions [41]. Polymer-bound chloramine-T (iodobeads) and Iodogen® (Iodogen®-coated tubes) were used as mild oxidizing agents. The radiochemical yield was determined via radio-TLC, and is presented as the percentage of the desired radiolabeled product **Boc-[^{124}I]CKIA** in the reaction mixture at different time points.

The results in Table 1 clearly demonstrate the importance of precursor amount on the radiochemical yield. The use of 20 µg of trimethylstannyl compound **6** gave only low radiochemical yields of 30% after 30 min (entry 1). Increase of the amount of **6**–40 µg (entry 2) and 50 µg (entry 3) resulted in an improved radiochemical yield of 70% and 80%, respectively, after 30 min. Thus, a minimum of 40 µg of labeling precursor seems to be necessary to achieve reasonable radiochemical yields. Further increase of the amount of compound **6**–100 µg (entry 4) gave the desired radiolabeled compound **Boc-[^{124}I]CKIA** in radiochemical yields of 82% after 10 min, 89% after 20 min, and very good 94% after 30 min. The use of more oxidizing agent (2 iodobeads, entries 4 and 6) did not further improve the radiochemical yield. The use of 200 µg of labeling precursor **6** afforded 90% of radiolabeled compound **Boc-[^{124}I]CKIA** after 10 min. The radiochemical yield could slightly be improved over time, reaching 93% after 20 min, and 95% after 30 min.

In addition to the use of immobilized chloramine-T as the oxidizing agent we also tested the reaction according to the Iodogen® method using Iodogen®-coated tubes (entry 8). The use of 40 µg of labeling precursor **6** gave radiochemical yield of 20% after 10 min and 25% after 20 min. Further extension of the reaction time to 30 min increased the radiochemical yield to 80%.

All reactions were stopped by the addition of 50 µl of saturated bisulfite solution to the reaction mixture. The radioiodination step proceeded without formation of any by-products as monitored by radio-TLC. Since the oxidation agent is immobilized (iodobeads or Iodogen®-coated tubes) it can easily be separated from the reaction mixture for the subsequent deprotection step of the Boc group.

Table 1
Radiolabeling of compound **6** with [^{124}I]NaI.

Entry	Mass	Oxidizing agent	Radiochemical yield [%]		
			10 min	20 min	30 min
1	20 µg	1 Iodobead	18	20	30
2	40 µg	1 Iodobead	58	58	70
3	50 µg	1 Iodobead	55	58	80
4	60 µg	2 Iodobeads	40	52	64
5	100 µg	1 Iodobead	82	89	94
6	100 µg	2 Iodobeads	56	81	91
7	200 µg	1 Iodobead	90	93	95
8	40 µg	Iodogen®	20	25	80

For a larger scale radiosynthesis (40 MBq–275 MBq of [^{124}I]NaI), 250 μg of labeling precursor **6** dissolved in 50 μl of solvent precursor was used. However, the use of iodobeads as the oxidizing agent caused unexpected problems. Most of the radioactivity was irreversibly attached to the iodobeads. Attempts to remove the product from the iodobeads by means of various solvents such as diethyl ether, chloroform, ethyl acetate and methanol, failed. For this reason, we decided to perform the reaction with Iodogen®-coated tubes. The use of the Iodogen® method in Iodogen®-coated tubes proved to be the approach of choice. No undesired loss of activity was observed. The reaction mixture was incubated at room temperature for 10 min. Radio-TLC analysis indicated product formation of greater than 90%. The reaction mixture was quenched by the addition of 50 μl of saturated sodium bisulfite. Deprotection was performed with trifluoroacetic acid (TFA) at 50 °C. Removal of the Boc protecting group was accomplished after 20 min to give the desired compound **[^{124}I]CKIA** in radiochemical yields of 45–65% along with the formation of some not further identified side products (≤40%). Lowering the reaction temperature to 25 °C resulted in significantly lower radiochemical yield (13%) of the desired product but with also significantly lower amounts of side products (7%). Increasing the reaction temperature of the deprotection step to 90 °C resulted in complete deprotection of compound **Boc-[^{124}I]CKIA** leading to the formation of 60% of compound **[^{124}I]CKIA** along with 40% of side products. The results are summarized in Table 2.

The crude product was subjected onto a semi-preparative HPLC column for purification. The product fraction (13.2–14.0 min) was collected, diluted with water and passed through a Waters Sep-Pak-tC-18 cartridge. The cartridge was washed with water and the final product **[^{124}I]CKIA** was eluted with 1 mL ethanol. The solvent was evaporated in a gentle stream of nitrogen to afford compound **[^{124}I]CKIA** in radiochemical yield of 33.6%. Optimized reaction conditions were also applied to the synthesis of compound **[^{124}I]CKIB**, which was prepared in radiochemical yield of 28%. The specific activity was determined to be 35 GBq/μmol for compound **[^{124}I]CKIA** and 25 GBq/μmol for compound **[^{124}I]CKIB**. The radiochemical purity of both compounds exceeded 95% suitable for further radiopharmacological characterization.

2.2. Lipophilicity

Lipophilicity (log *D* at pH = 7.4) is an important and fundamental physico-chemical property of a compound in the area of rational drug design and development. It is a key parameter of structure-activity relationship studies in medicinal chemistry to predict cell membrane penetration and blood protein binding. In the field of radiotracer design and development, lipophilicity is often used to predict delivery of the radiotracer to target tissues or organs, and to anticipate the clearance rate of the radiotracer from non-target tissue [42,43]. In the case of compounds **[^{124}I]CKIA** and **[^{124}I]CKIB** as potential Cdk4 inhibitors, the radiotracer should possess an appropriate lipophilicity to enable sufficient cell uptake while avoiding undesired high non-specific binding to plasma proteins.

The lipophilicity of both radiotracers was measured according to the method reported by Wilson et al. [43]. Compound **[^{124}I]CKIA** showed a log *D* value of 2.77 ± 0.13, whereas a lower log *D* of 1.99 ± 0.03 was determined for compound **[^{124}I]CKIB** at a pH-value of 7.4. Thus, substitution of the phenyl ring in compound **[^{124}I]CKIA** with a pyridine ring as in compound **[^{124}I]CKIB** resulted in a significant decrease of lipophilicity in the order of almost one magnitude.

2.3. Stability analysis

The stability of both radiotracers was tested in ethanol, buffer solution (PBS, pH 7.4), cell culture medium, and rat plasma at 37 °C at 30 min and 24 h with radio-HPLC. The results are summarized in Table 3.

Radio-HPLC analysis showed no substantial decomposition of both radiotracers after incubation in all media at 37 °C after 30 min. Comparable results were obtained after 24 h, with a more pronounced tendency for decomposition (14%) of compound **[^{124}I]CKIA** in buffer at 24 h. For all other media, high stability (>92%) of both compounds was found at 30 min and 24 h

2.4. Cell uptake studies

In vitro radiotracer cell uptake studies using **[^{124}I]CKIA** and **[^{124}I]CKIB** showed substantial uptake in HT-29 and FaDu tumor cells (approximately 750–850 %ID/mg protein **[^{124}I]CKIA** and 900–1000 %ID/mg protein **[^{124}I]CKIB** (means) after 1 h) at 37 °C (Fig. 3 A and B). In both cell lines HT-29 and FaDu the time-dependent cellular uptake of **[^{124}I]CKIA** and **[^{124}I]CKIB** was similar. The early uptake kinetics of both compounds was comparable in both tumor cell lines. In posterior phase (>1 h) **[^{124}I]CKIA** showed a further increasing cellular uptake compared to **[^{124}I]CKIB**. On the other hand, **[^{124}I]CKIB** uptake level remained nearly constant after 1 h. This is consistent with the different therapeutic potency of **CKIA** and **CKIB** observed in cell-cycle studies of tumor cell lines. Uptake of both radiolabeled compounds **[^{124}I]CKIA** and **[^{124}I]CKIB** could be blocked with non-radioactive **CKIA** or respectively **CKIB** in FaDu cells dependent on concentration (Fig. 3C), indicating a specific uptake mechanism.

2.5. Tissue biodistribution studies

The distribution of radiotracers **[^{124}I]CKIA** and **[^{124}I]CKIB** in selected tissues and organs was studied in normal Wistar rats at 5 min *p*.i. as relevant for the perfusion phase, and 60 min *p*.i. as relevant for the metabolic phase. The dose of both radiotracers was in the range of 0.2–0.3 MBq/animal. The results of the standardized radioactivity concentrations in different organs and tissues are presented in Fig. 4.

[^{124}I]CKIA and **[^{124}I]CKIB** showed similar biodistribution profiles, although they exhibit different lipophilicity at pH of 7.4 (log *D* = 2.77 for **[^{124}I]CKIA** and log *D* = 1.99 for **[^{124}I]CKIB**). High initial radioactivity concentrations after 5 min *p*.i. were detected in the lung (8.67 ± 2.04 for **[^{124}I]CKIA** and 8.43 ± 0.66 for **[^{124}I]CKIB**). High initial uptake values were also found in the spleen, adrenals,

Table 2
Radiochemical yields for Boc group removal after 30 min.

Compound	Radiochemical yield		
	25 °C	50 °C	90 °C
[^{124}I]CKIA	13%	45–65%	60%
Boc-[^{124}I]CKIA	80%	≤10%	0%
Side-products	7%	≤40%	40%

Table 3
Stability of **[^{124}I]CKIA** and **[^{124}I]CKIB** in different media.

Compound	EtOH		PBS buffer (pH 7.4)		Cell culture medium	Rat plasma	
	30 min	24 h	30 min	24 h	24 h	30 min	24 h
[^{124}I]CKIA	93%	94%	92%	86%	96%	93%	94%
[^{124}I]CKIB	98%	97%	97%	95%	97%	94%	94%

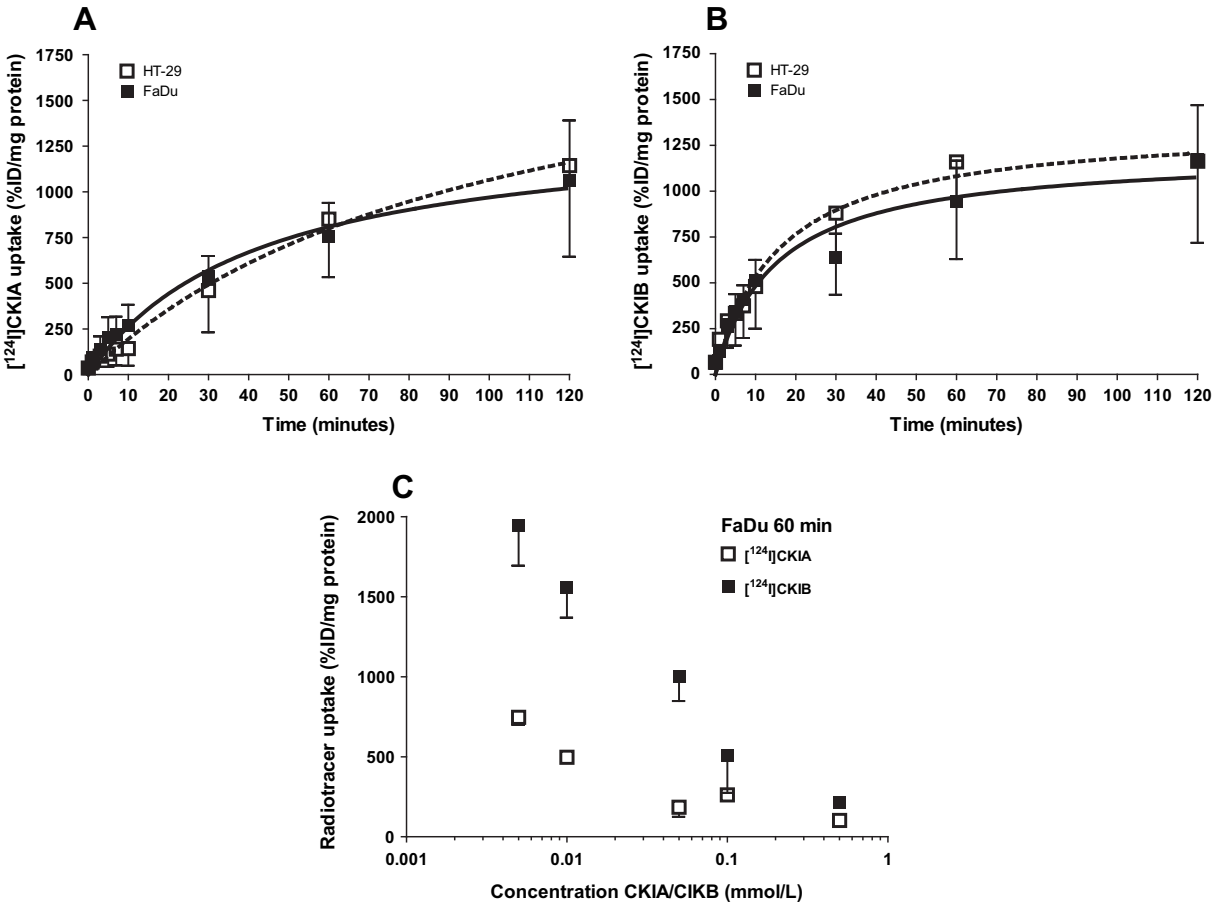

Fig. 3. Cellular radiotracer uptake of [^{124}I]CKIA (A) and [^{124}I]CKIB (B) over a period of 2 h at 37 °C and blocking experiments with different concentrations non-radioactive CKIA or CKIB, respectively, in FaDu after 60 min at 37 °C (C) (means ± SD, $n \geq 8$, ANOVA).

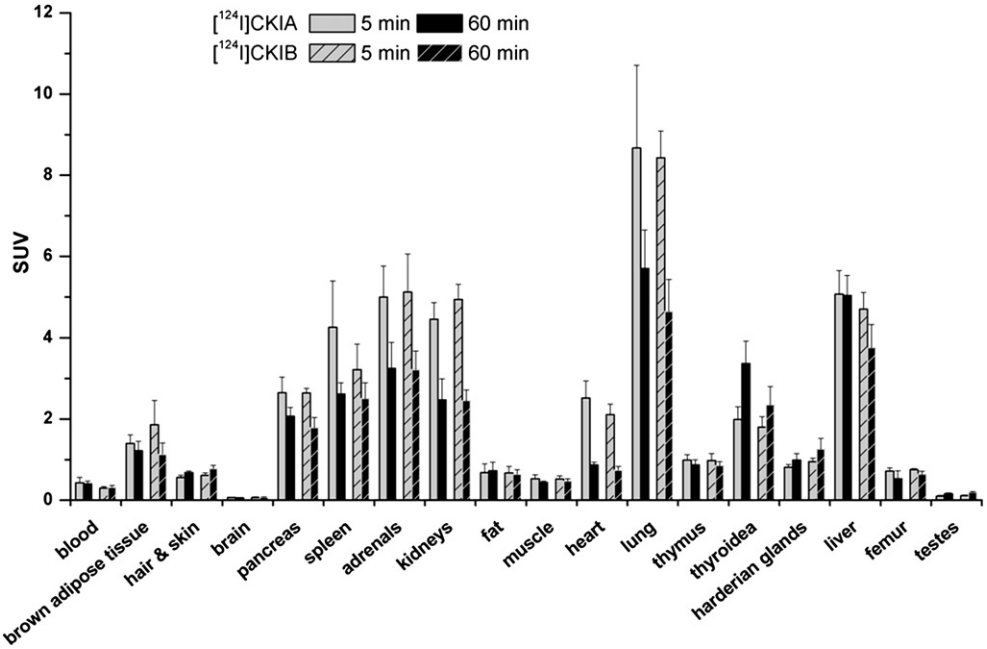

Fig. 4. Biodistribution of [^{124}I]CKIA or [^{124}I]CKIB in selected tissues and organs of normal male Wistar rats (body weight 180 ± 20 g) after single intravenous injection at 5 min and 60 min. Data are presented as standardized uptake values (SUV). SUV = (organ activity/organ weight)/(total given activity/rat body weight)/(Bq/g); means ± SD; $n = 8$.

kidneys and liver (SUV > 3.2) after 5 min *p*.i. The initial high radioactivity uptake in these organs was decreased at 60 min *p*.i. in the case of less lipophilic compound **[^{124}I]CKIB**, whereas more lipophilic radiotracer **[^{124}I]CKIA** did not clear from the liver after 60 min *p*.i.

No radioactivity uptake was found in the brain at 5 min and 60 min *p*.i. suggesting that both radiotracers do not sufficiently penetrate the blood–brain barrier, and/or that they are substrates for the P-glycoprotein efflux pump. Radioactivity was cleared from most organs and tissues within 60 min after radiotracer administration, except for thyroidea. The observed increase of radioactivity concentration in the thyroidea is indicative of an *in vivo* radiodeiodination and accumulation of free [^{124}I]iodide in the thyroidea over time. The determined biodistribution profile of both radiotracers suggests a predominantly hepatobiliary elimination pathway.

2.6. In vivo stability

Metabolic stability *in vivo* of radiotracers **[^{124}I]CKIA** and **[^{124}I]CKIB** was studied in rats. Fig. 5 shows the time curves of the percentage of original compound at different time points in rat blood plasma after single intravenous injection.

Both radiotracers showed similar metabolic stability profiles indicating that both compounds are rapidly metabolized *in vivo*. After 10 min, a fraction of 19% (**[^{124}I]CKIA**) and 21% (**[^{124}I]CKIB**), respectively, of intact parent compound was detected. Two new more hydrophilic peaks appeared, which have not been characterized further. Both radiotracers were almost completely metabolized after 60 min *p*.i., resulting in a remaining fraction of intact parent compounds of less than 5%. However, the found SUV values of 3.2 (**[^{124}I]CKIA**) and 2.2 (**[^{124}I]CKIB**) for thyroids from the tissue biodistribution study at 60 min *p*.i. (Fig. 4) suggest, that radiodeiodination seems not to be the main catabolic pathway. Obviously, the shown instability of both compounds *in vivo* is an obstacle for performing *in vivo* analyses. The *in vivo* stability was unexpectedly low despite the high *in vitro* stability shown in Table 3. Further investigations should deal with the identification of the two new formed metabolites in order to gain information for stabilizing this compounds.

2.7. Small-animal PET imaging and ex vivo autoradiography

To further assess the metabolic pathway of radiotracers **[^{124}I]CKIA** and **[^{124}I]CKIB**, small-animal PET imaging was performed in FaDu xenograft bearing mice as models of human tumors. Representative images for both tumor models are shown in Fig. 6.

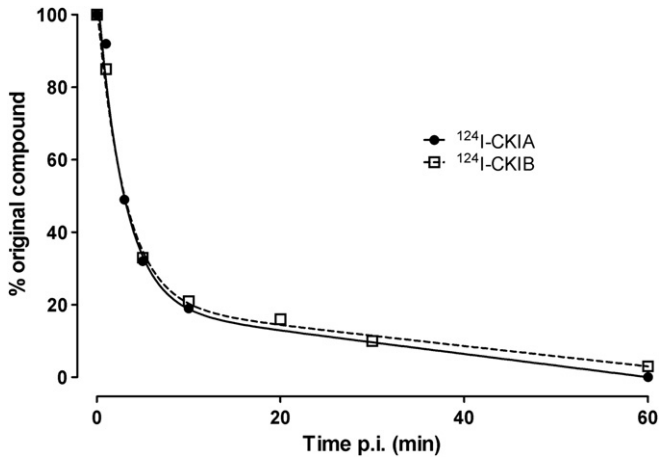

Fig. 5. Representative curves of original [^{124}I]CKIA and [^{124}I]CKIB in rat blood plasma as percentage of the total plasma activity from two rats after single intravenous injection.

The maximum intensity projections at different time points further confirm the comparable biodistribution pattern for **[^{124}I]CKIA** and **[^{124}I]CKIB** in FaDU tumor-bearing mice, as found in the biodistribution studies with rats. Both radiotracers were predominantly hepatobiliarly eliminated, with no specific radioactivity accumulation in other organs and tissues, including the tumor.

Time activity curves of radiotracers **[^{124}I]CKIA** and **[^{124}I]CKIB** demonstrated rapid clearance of both compounds from the blood, and accumulation of radioactivity in the liver and thyroid over time (Fig. 7). More lipophilic compound **[^{124}I]CKIA** (log D = 2.77, pH = 7.4) showed higher liver uptake compared with less lipophilic compound **[^{124}I]CKIB** (log D = 1.99, pH = 7.4).

The half-life of radioactivity clearance from the blood was calculated according to a two-phase distribution profile, derived from ROI's over the heart, which is representative of the radioactivity clearance from the blood. The data were not partial volume corrected. The calculated half-life accounting for the late phase was 7.3 min in the case of compound **[^{124}I]CKIA** and 6.4 min for compound **[^{124}I]CKIB**. The half-times accounting for the early distribution phase were 21 s and 26 s for **[^{124}I]CKIA** and **[^{124}I]CKIB**, respectively.

Biodistribution profile of both radiotracers in FaDu tumor-bearing mice was further studied by ex vivo autoradiography. Representative autoradiograms at 60 min after radiotracer administration and the corresponding histological sections are given in Fig. 8. Highest radioactivity concentrations were observed in the liver and intestine for both compounds. No radioactivity was found in the brain and only marginal uptake in the FaDu tumor. These finding are consistent with the results obtained from the biodistribution and small-animal PET studies.

3. Conclusions

The radiosynthesis of two ^{124}I-labeled Cdk4 inhibitors has been developed. Both non-carrier added radiotracers were obtained in reproducible radiochemical yields and purity enabling detailed radiopharmacological characterization. *In vitro* experiments demonstrated substantial cellular uptake in tumor cell lines HT-29 and FaDu and a high *in vitro* stability in rat plasma and cell culture medium. In contrast, small-animal PET and autoradiography studies *in vivo* showed only very low uptake in FaDu tumors due to a rather low *in vivo* stability. So both radiolabeled compounds show limitations regarding their ability to act as a radiotracer for imaging of tumor cells *in vivo*. On the other hand, the corresponding non-radioactive compounds clearly show inhibitory effects on cell-cycle regulation in the tumor cells when applied in pharmacological concentrations (50 nM–1 μM) as shown previously by our group [44]. The analysis of the metabolic fate of the compounds *in vivo* should come to the fore to develop more stable compounds enabling the imaging of tumor cells *in vivo*. Further studies should also focus on the development of more hydrophilic and, regarding the positron-emitting nuclide, fluorine-18 radiolabeled derivatives of **CKIA** and **CKIB** as suitable radiotracers for imaging Cdk4 by means of PET.

4. Materials and methods

4.1. General methods

All reagents and solvents were purchased from commercial suppliers and used without further purification unless otherwise

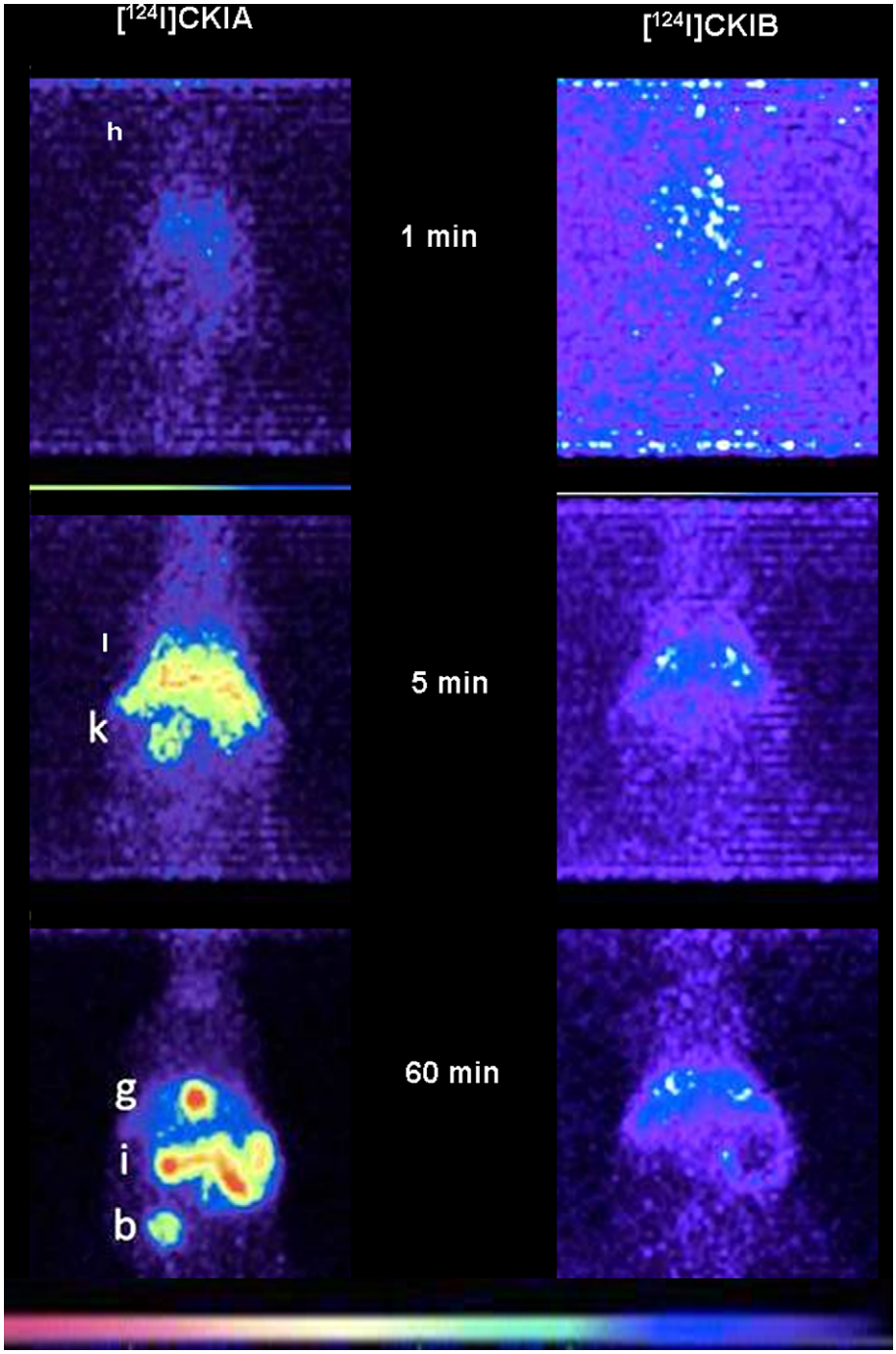

Fig. 6. Maximum intensity projections of small-animal PET studies with [^{124}I]CKIA and [^{124}I]CKIB in FaDu tumor-bearing mice at 1 min, 5 min and 45 min midframe time after single intravenous injections (b: bladder; g: gall bladder; h: heart; i: intestines; k: kidneys; l: liver).

specified. Iodogen® precoated tubes were purchased from Thermo Scientific Pierce Protein Research Products, Iodo-Beads were purchased from Sigma–Aldrich. [^{124}I]NaI (3 MBq/μl, 0.1 M sodium hydroxide solution) in 3 mL KIMAX V vials was purchased from QSA Global GmbH (Braunschweig, Germany). NMR spectra were recorded on a Varian Inova 400 MHz spectrometer. ^{1}H chemical shifts are given in ppm and were referenced with the residual solvent resonances relative to tetramethylsilane (TMS). Mass spectra (MS) were obtained on a Quattro/LC mass spectrometer (MICROMASS) using electrospray ionization. Silica-gel column chromatography was performed on MERCK silica-gel 60 (mesh size 230–400 ASTM). Reactions were monitored by thin-layer chromatography (TLC) on Merck silica-gel 60 F-254 aluminum plates, with visualization under UV (254 nm). Radio-TLC analyses was performed on Merck silica-gel RP-18 aluminum plates and Merck silica-gel 60 F-254 aluminum plates, with visualization using a Fuji 2000 BAS reader and AIDA (Advanced Image Data Analyzer, version 4.10.020) software. Melting points were determined with a Galen III™ melting point apparatus from Cambridge Instruments. The following compounds were prepared according to literature procedures: 8-cyclopentyl-6-iodo-5-methyl-2-(methylsulfinyl)-pyrido[2,3-*d*]pyrimidin-7(**8*H***)-one **1** [36], *tert.*-butyl 4-(4-aminophenyl)piperazine-

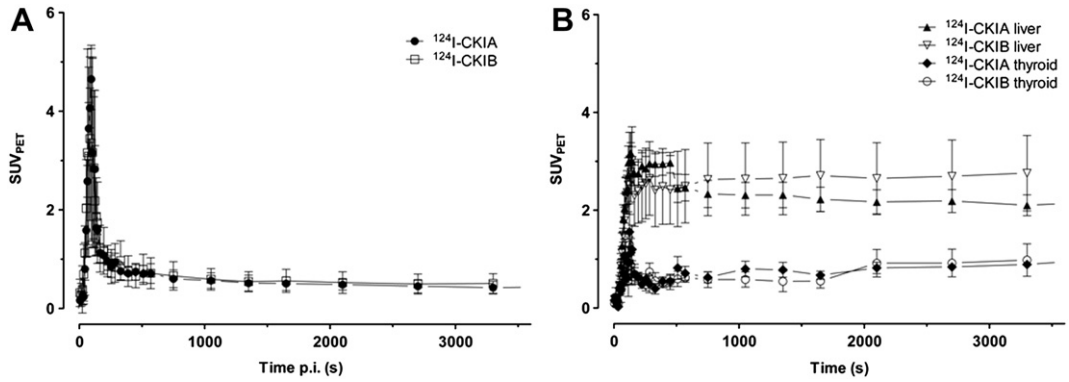

Fig. 7. Time activity curves of radioactivity concentration from ROI's over the heart (A), and liver and thyroid (B) of [^{124}I]CKIA and [^{124}I]CKIB in FaDu tumor-bearing mice after single intravenous injections. Data are expressed as SUV$_{PET}$ (means ± SD, $n = 4$).

1-carboxylate **2** [36] and *tert*.-butyl-4-(4-aminopyridin-3-yl)piperazine-1-carboxylate **3** [34]. High performance liquid chromatography (HPLC) analyses (VWR-Hitachi Elite LaChrom system) were carried out with a Supelco RP-18 column (Supelco Discovery C18 4.6 × 150 mm, 5 μm) using a gradient elution with 0.1% trifluoroacetic acid (TFA)/CH_3CN (containing 0.1% TFA) from a gradient pump (VWR Hitachi Elite-LaChrom Pump L-2130) (**[^{124}I]CKIA**: 0 min 60/40, 7 min 60/40, 12 min 20/80, 16 min 20/80; **[^{124}I]CKIB**: 0 min 70/30, 5 min 70/30, 10 min 20/80, 12 min 20/80) using a flow of 1 mL/min. The products were monitored by an UV

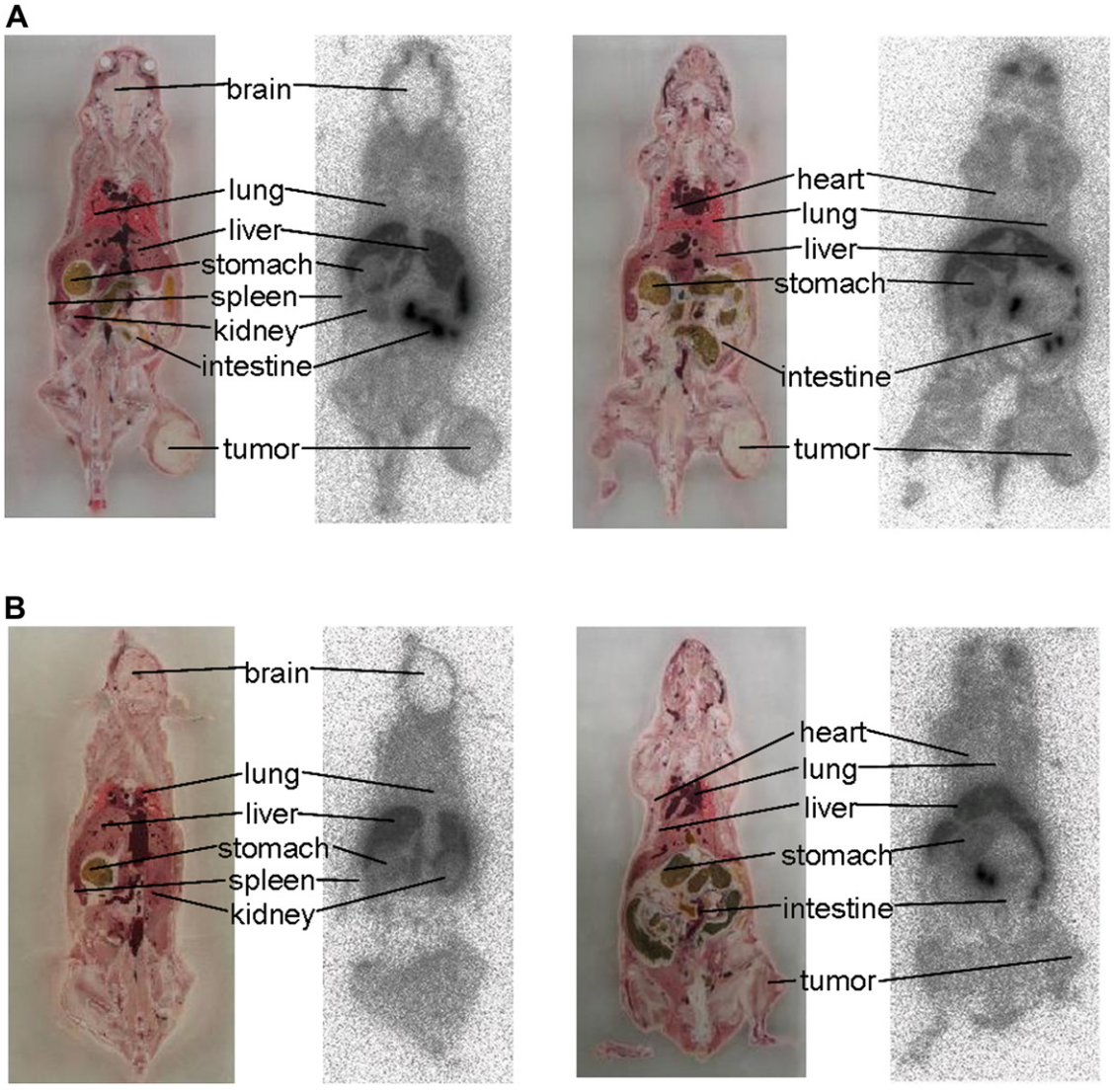

Fig. 8. Representative ex vivo autoradiograms at 60 min after injection of [^{124}I]CKIA (A) and [^{124}I]CKIB (B), and the corresponding histological sections.

detector (VWR Hitachi Elite-LaChrom UV/VIS detector L-2400) at 270 nm and by γ-detection with a scintillation detector Gabi (raytest). Semi-preparative HPLC purification was performed on a Supelco RP-18 column (Supelco Discovery C18) 10 × 250 mm, 5 μm) using gradient elution (Jasco LG 2080-02 Ternary Gradient Unit) with CH_3CN (containing 0.1% TFA)/0.1% TFA (0 min 40–60, 20 min 40/60, 30 min 80/20, 50 min 80/20) at a flow rate of 3.0 mL/min for **[^{124}I]CKIA** and 1.5 mL/min for **[^{124}I]CKIB** (Jasco PU-2080plus Intelligent Pump System). The products were monitored by an UV detector (Jasco UV-2075 plus intelligent UV/VIS detector) at 270 nm and by γ-detection with a scintillation detector Robotron 20 046.

4.2. Chemical synthesis

4.2.1. General procedure for the introduction of the side chains 2 and 3 to sulfoxide 1 at C2 position

Sulfoxide **1** (420.0 mg, 1.00 mmol) and *tert.*-butyl 4-(4-aminophenyl)piperazine-1-carboxylate **2** or *tert.*-butyl-4-(4-aminopyridin-3-yl)piperazine-1-carboxylate **3** (1.1 mmol) were dissolved in DMSO (5 mL) for synthesis of compound **4** and toluene (5 mL) for the synthesis of compound **5** and heated at 100 °C for 16 h. The reaction mixture was cooled to room temperature, diluted with brine and extracted with ethyl acetate. The organic layer was dried over sodium sulfate and filtered. The filtrate was concentrated in vacuum to give compounds **4** and **5** as yellow–orange solids. The products were used for the next reaction steps without further purification.

tert-Butyl-4-(6-(8-cyclopentyl-6-iodo-5-methyl-7-oxo-7,8-dihydro-pyrido[2,3-*d*]pyrimidin-2-ylamino)phenyl)piperazine-1-carboxylate (4). Yield: 75%. ^{1}H NMR ($CDCl_3$, 400 MHz) δ 8.72 (s, 1H), 7.47 and 6.95 (2d of AA'BB' system, J = 8.8 Hz, 4H, Ar-H), 5.97 quint., J = 8.4 Hz, 1H), 3.63–3.58 (m, 4H), 3.15–3.08 (m, 4H), 2.66 (s, 1H, CH_3), 2.30–2.22 (m, 2H), 2.06–1.98 (m, 2H), 1.87–1.78 (m, 2H), 1.68–1.56 (m, 2H), 1.49 (s, 9H). Low-resolution mass spectrometry electron spray ionization (ESI^+): 631.4 [M + H].

tert-Butyl-4-(6-(8-cyclopentyl-6-iod-5-methyl-7-oxo-7,8-dihydropyrido[2,3-*d*]pyrimi-din-2-yl-amino)pyridin-3-yl)piperazine-1-carboxylate (5). Yield: 38%. ^{1}H NMR ($CDCl_3$, 400 MHz) δ 9.41 (s, 1H, CH); 8.11 (m, 1H), 7.92 (m, 1H), 7.83 (m, 1H), 6.46–6.36 (m, 1H), 3.74 (m, 4H), 3.66 (m, 4H), 2.98 (s, 3H, CH_3), 2.50–2.40 (m, 2H) 2.33–2.23 (m, 2H), 2.14–2.04 (m, 2H), 1.93–1.83 (m, 2H), 1.49 (s, 9 H, $(CH_3)_3$). Low-resolution mass spectrometry electron spray ionization (ESI^+): 632.4 [M + H].

4.2.2. General procedure for removal of the Boc protecting group

Compound **4** or **5** (0.44 mmol) was stirred at ambient temperature in dioxane (4 mL) and 6 M HCl (4 mL) for 2 h. The solvent was evaporated in vacuum, and the residue was diluted with methanol. The product was precipitated by adding diethyl ether. The resulting solids were filtrated off and re-dissolved in dichloromethane. The product was purified by silica-gel chromatography ($MeOH/CHCl_3$ 1/1) to give compounds **CKIA** and **CKIB** as greyish-yellow solids.

8-Cyclopentyl-6-iod-5-methyl-2-(4-(piperazin-1-yl)phenylamino)-pyrido[2,3-*d*]pyri-midin-7(8H)-one (CKIA). Yield: 95%. m_p = 200–201 °C. ^{1}H NMR (acetone, 400 MHz) δ 9.25 (br, s, 1H); 8.90 (s, 1H), 7.59 (d, 2H, J = 9.0 Hz, Ar-H), 7.03 (d, 2H, J = 9.0 Hz, Ar-H), 5.95–5.85 (m, 1H), 3.35–3.31 (m, 4H), 3.25–3.20 (m, 4H), 2.63 (s, 3H), 2.20–2.10 (m, 2H), 1.95–1.85 (m, 2H), 1.80–1.70 (m, 2H), 1.54–1.52 (m, 2H). Low-resolution mass spectrometry electron spray ionization (ESI^+): 531.2 [M + H].

8-Cyclopentyl-6-iodo-5-methyl-2-(5-(piperazin-1-yl)pyridin-2-ylamino)pyrido[2,3-*d*]pyrimidin-7(8H)-one (CKIB). Yield: 95%. m_p > 240 °C. ^{1}H NMR (acetone, 400 MHz) δ 9.15 (s, 1H); 8.25–8.20 (m, 1H), 7.99–7.96 (m, 1H), 7.55–7.51 (m, 1H), 6.11–6.05 (m, 1H), 3.55–3.51 (m, 4H), 3.45–3.40 (m, 4H), 2.80 (s, 3H), 2.24–2.16 (m, 2H), 2.12–2.04 (m, 2H), 1.92–1.80 (m, 2H), 1.72–1.64 (m, 2H). Low-resolution mass spectrometry electron spray ionization (ESI^+): 532.3 [M + H].

4.2.3. General procedure for the synthesis of trimethyl stannyl-containing compounds

Under nitrogen, hexamethyl distannane (0.617 mmol) and tetrakis(triphenyl-phosphine)palladium(0) (0.024 mmol) were dissolved in dioxane (10 mL). Compound **4** or **5** (0.475 mmol) was added, and the reaction mixture was refluxed for 8 h. The reaction mixture was cooled to room temperature, and the solvent was evaporated in vacuum. The residue was the purified by silica-gel chromatography (ethyl acetate/petroleum ether 1/1) to yield **6** and **7** as greyish-yellow solids.

tert-Butyl-4-(6-(8-cyclopentyl-5-methyl-7-oxo-6-trimethylstannyl-7,8-dihydro-pyrido[2,3-d]pyrimidin-2-ylamino)phenyl)piperazine-1-carboxylate (6). Yield: 32%. m_p = 225–227 °C. ^{1}H NMR ($CDCl_3$, 400 MHz) δ 8.59 (s, 1H), 7.42 (d, 2H, J = 8.9 Hz, Ar-H), 6.92 (d, 2H, J = 9.0 Hz, Ar-H), 5.73–5.69 (m, 1H), 3.68 (s, 3H), 3.60–3.55 (m, 4H), 3.10–3.06 (m, 4H), 2.235–2.25 (m, 2H), 1.90–1.70 (m, 4H), 1.65–1.55 (m, 2H), 1.43 (s, 9H), 0.36 (s, 9H). Low-resolution mass spectrometry electron spray ionization (ESI^+): 669.3 [M + H].

tert.-Butyl-4-(6-(8-cyclopentyl-5-methyl-7-oxo-6-trimethylstannyl-7,8-dihydro-pyrido[2,3-*d*]pyrimidin-2-ylamino)pyridin-3-yl)piperazine-1-carboxylate (7). Yield: 55%. m_p = 209–211 °C. ^{1}H NMR ($CDCl_3$, 400 MHz) δ 8.70 (s, 1H, CH); 8.27–8.20 (m, 1H), 8.02–7.99 (m, 1H), 7.81–7.75 (m, 1H), 5.82–5.71 (m, 1H), 3.72 (s, 3H), 3.67–3.58 (m, 4H), 3.17–3.09 (m, 4H), 2.09–1.98 (m, 4H), 1.90–1.78 (m, 2H), 1.74–1.64 (m, 2H), 1.49 (s, 9H), 0.36 (s, 9H). Low-resolution mass spectrometry electron spray ionization (ESI^+): 670.3 [M + H].

4.3. Radiosynthesis

Preparation of [^{124}I]CKIA. 50 μl of **6** (5 μg/μl in DMSO/5% HOAc in MeOH 1/3) was placed in a iodotube followed by the desired quantity of **[^{124}I]NaI** (36.08 MBq, ca. 3 MBq/μl in 0.1 M sodium hydroxide). The reaction mixture was diluted with 100 μl of 5% glacial acetic acid in methanol. The Iodotube was shaken for 10 min at room temperature. After 10 min the conversion was monitored via radio-TLC. The reaction was quenched with 50 μl saturated sodium bisulfite and transferred into a low-bind eppendorf vial. 200 μl trifluoroacetic acid was added. After shaking for 20 min at 50 °C the crude product was subjected onto a semi-preparative HPLC column. The product fraction (13.2–14.0 min) was collected, diluted with water (20 mL) and passed through a Waters Sep-Pak tC-18 cartridge. The cartridge was washed with water (10 mL) and **[^{124}I]CKIA** was eluted with ethanol (1 mL). The solvent was evaporated in a gentle stream of nitrogen to afford 11.8 MBq (33.6%, decay-corrected) of **[^{124}I]CKIA** within 104 min, including HPLC purification. The specific activity was determined to be 35 GBq/μmol. Radio-HPLC-analysis: t_R = 5.9 min.

Preparation of [^{124}I]CKIB. Starting from 50 μl of **7** (5 μg/μl in DMSO/5% HOAc in MeOH 1/3) and **[^{124}I]NaI** (186.1 MBq, ca. 3 MBq/μl in 0.1 M sodium hydroxide) 32.66 MBq (17.8%, decay-corrected) of **[^{124}I]CKIB** was obtained according to the method described for radiosynthesis of **[^{124}I]CKIA** within 107 min, including HPLC purification. The specific activity was determined to be 25 GBq/μmol. Radio-HPLC-analysis: t_R = 4.2 min.

4.4. Lipophilicity

Lipophilicity (log D) of **[^{124}I]CKIA** and **[^{124}I]CKIB** was determined at pH 7.4 according to the method reported by Wilson et al. [43].

4.5. Stability studies

In vitro and ex vivo stability studies of the radiotracers **[^{124}I]CKIA** and **[^{124}I]CKIB** were performed by HPLC analysis. The radiolabeled compounds (50 kBq) were added to 1 mL of phosphate buffered saline (PBS, 0.1 M, pH 7.4), ethanol, cell culture medium (RPMI + 10% FKS + 1% penicillin/streptomycin) or fresh rat plasma and were incubated for 30 min or 24 h at 37 °C. HPLC analysis was performed on a Hewlett Packard Series 1100 (detector: Raytest Ramona) with a Zorbax 300SB-C18 column (250 × 9.4 mm, 5 μm) using a gradient elution with Soerensen buffer (0.01 M, pH 7.4) and methanol (in 5 min from 40 to 90% methanol, then 25 min 90% methanol) by injection of the samples.

4.6. Biological studies

4.6.1. Cellular studies

Human tumor cell lines HT-29 (a colorectal adenocarcinoma cell line), and FaDu (a head and neck squamous cell carcinoma cell line) were cultured in McCoy's 5A medium (HT-29) or RPMI 1640 medium (FaDu) supplemented with 10% fetal bovine serum (FBS) and 1% penicillin-streptomycin at 37 °C, 5% CO_2 and 95% humidity in a CO_2 incubator (Heracell, Heraeus, Hanau, Germany).

For radiotracer uptake experiments, 5×10^4 cells were seeded in a cavity of a 24 well plate (Greiner, Frickenhausen, Germany). After overnight incubation, 0.25 mL of cell culture medium with about 25 kBq of **[^{124}I]CKIA** or **[^{124}I]CKIB** was added, and incubation was continued for several time points at 37 °C. Subsequently, cells were washed three times with ice-cold PBS and lysed in 0.5 mL of 0.1 M sodium hydroxide with 1% SDS. Cell lysates were counted with a Cobra II gamma counter (Canberra-Packard, Meriden, CT, USA). Protein levels were quantified using the BCA protein assay kit (Pierce, Rockford, USA) according to the manufacturer's recommendations and bovine serum albumin as protein standard. Uptake data for all experiments are expressed as percent of injected dose per mg protein (%ID/mg protein).

4.6.2. Biodistribution studies

Biodistribution of radiotracers **[^{124}I]CKIA** and **[^{124}I]CKIB** were studied in male Wistar rats (Unilever, Harlan Germany, 200–230 g body weight) after 5 min and 60 min post injection. Aliquots (0.2–0.3 MBq) of each compound were added to 500 μl of E153 infusion solution containing 1% HSA, and the solution was administered intravenously into the tail vein. After radiotracer application, rats were anaesthetized with ether at 5 or 60 min *p.i.*, respectively. Afterwards, blood samples were withdrawn by heart puncture, and the animals were euthanized. Organs and tissues were removed and weighted, and the radioactivity was measured in a calibrated well counter. The data were normalized to the amount of injected radioactivity, and expressed as standardized uptake values (SUV, SUV = (organ activity/organ weight)/(total given activity/rat body weight)).

4.6.3. Small-animal PET imaging and ex vivo autoradiography

Small-animal positron emission tomography experiments were performed on an established mouse tumor xenograft model (NMRI nu/nu male mice with implanted FaDu tumor, transplantation procedure described in ref. [45]).

When tumors reached a weight of about 200 mg, imaging studies were performed on a dedicated small-animal PET scanner (microPET P4; CTI Concorde Microsystems). The animals were anesthetized through inhalation of 9% desflurane (v/v) (Suprane; Baxter) in 40% oxygen/air (gas flow, 1 L/min). Then, the animals were positioned and immobilized prone with their medial axis parallel to the axial axis of the scanner and their thorax, abdomen, and hind legs (organs of interest: liver and tumor) in the center of the field of view. For attenuation correction, a 15 min transmission scan was performed using a rotating ^{57}Co point source before tracer injection and collection of the emission scans. Then, approximately 10 MBq of **[^{124}I]CKIA** and **[^{124}I]CKIB** were administered intravenously within 15 s in a 0.3 mL volume into the tail vein. Simultaneously with tracer application, PET measurement was started for 60 min. Sinogram generation and image reconstruction followed the protocol reported by our group elsewhere [46]. Three-dimensional tumor regions of interest were determined for subsequent data analysis. As an index of **[^{124}I]CKIA** or respectively **[^{124}I]CKIB** uptake *in vivo*, maximum standardized uptake values (SUVs) at 60 min after injection were calculated in regions of interest for each PET measurement. The SUV value, expressing the ratio of **[^{124}I]CKIA** or **[^{124}I]CKIB** uptake in relation to the injected **[^{124}I]CKIA** or **[^{124}I]CKIB** activity normalized to body weight, was calculated using the Rover software package (ABX Radeberg).

After PET measurements, mice were euthanized and ex vivo autoradiography of whole mice was performed on a cryostat (Jung Cryopolycut, Leica)1 h after injection of radiotracers **[^{124}I]CKIA** and **[^{124}I]CKIB**. The body sections were dried in a freeze-dryer and then exposed to a phosphor imaging plate for 4 h and scanned (Bio Imaging Analyzer Fujifilm BAS-5000).

All animal experiments were performed in accordance with the guidelines of the German laws for animal Welfare. The protocol was approved by the local Ethical Committee for Animal Experiments.

Acknowledgements

The authors are grateful to Heidemarie Kasper, Regina Herrlich, Andrea Suhr and Mareike Barth for their excellent technical assistance.

References

[1] H.X. An, M.W. Beckmann, G. Reifenberger, H.G. Bender, D. Niederacher, Am. J. Clin. Pathol. 154 (1999) 113–118.
[2] S. Ortega, M. Malumbres, M. Barbacid, Biochim. Biophys. Acta. Rev. Cancer 1602 (2002) 73–87.
[3] A. Perry, K. Anderl, T.J. Borell, D.W. Kimmel, C.H. Wang, J.R. O'Fallon, B.G. Feuerstein, B.W. Scheithauer, R.B. Jenkins, Am. J. Clin. Pathol. 112 (1999) 801–809.
[4] G. Wei, F. Lonardo, T. Ueda, T. Kim, A.G. Huvos, J.H. Healey, M. Ladanyi, Int. J. Cancer 80 (1999) 199–204.
[5] D.G. Johnson, C.L. Walker, Annu. Rev. Pharmacol. Toxicol 39 (1999) 295–312.
[6] D.O. Morgan, Annu. Rev. Cell Dev. Biol. 13 (1997) 261–291.
[7] C.J. Sherr, Science 274 (1996) 1672–1677.
[8] T. Shimamura, J. Shibata, H. Kurihara, T. Mita, S. Otsuki, T. Sagara, H. Hirai, Y. Iwasawa, Bioorg. Med. Chem. Lett. 16 (2006) 3751–3754.
[9] J.A. Diehl, Cancer Biol. Ther. 1 (2002) 226–231.
[10] C.J. Sherr, Cell 73 (1993) 1059–1065.
[11] M. Malumbres, M. Barbacid, Trends Biochem. Sci. 30 (2005) 630–641.
[12] G.I. Shapiro, J. Clin. Oncol 24 (2006) 1770–1783.
[13] H.C. Thoms, M.G. Dunlop, L.A. Stark, Cell Cycle 6 (2007) 1293–1297.
[14] P.S. Sharma, R. Sharma, R. Tyagi, Curr. Cancer Drug Targets 8 (2008) 53–75.
[15] P.M. Fischer, Cell Cycle 3 (2004) 742–746.
[16] Y.M. Lee, P. Sicinski, Cell Cycle 5 (2006) 2110–2114.
[17] B.A. Carlson, M.M. Dubay, E.A. Sausville, L. Brizuela, P.J. Worland, Cancer Res. 56 (1996) 2973–2978.
[18] G. Kaur, M. Stetler-Stevenson, S. Sebers, P. Worland, H. Sedlacek, C. Myers, J. Czeck, R. Naik, E. Sausville, Nat. Cancer Inst. 84 (1992) 1736–1740.
[19] R.N. Misra, J. Med. Chem 47 (2004) 1719–1728.
[20] S. Akinaga, K. Gomi, M. Morimoto, T. Tamaoki, M. Okabe, Cancer Res. 51 (1991) 4888–4892.
[21] K. Kawakami, H. Futami, J. Takahara, K. Yamaguchi, Biochem. Biophys. Res. Commun. 219 (1996) 778–793.
[22] F.I. Raynaud, S.R. Whittaker, P.M. Fischer, S. McClue, M.I. Walton, S.E. Barrie, M.D. Garrett, P. Rogers, S.J. Clarke, L.R. Kelland, M. Valenti, L. Brunton, S. Eccles, D.P. Lane, P. Workman, Clin. Cancer Res. 11 (2005) 4875–4888.
[23] J. Vesely, L. Havlicek, M. Strnad, J.J. Blow, A. Donelladeana, L. Pinna, D.S. Letham, J. Kato, L. Detivaud, S. Leclerc, L. Meijer, Eur. J. Biochem. 224 (1994) 771–786.

[24] S.J. McClue, D. Blake, R. Clarke, A. Cowan, L. Cummings, P.M. Fischer, M. MacKenzie, J. Melville, J.K. Stewart, S. Wang, N. Zhelev, D. Zheleva, D.P.I. Lane, Int. J. Cancer 102 (2002) 463–468.
[25] B.P. Nutley, F.I. Raynaud, S.C. Wilson, P.M. Fischer, A. Hayes, P.M. Goddard, S.J. McClue, M. Jarman, D.P. Lane, P. Workman, Mol. Cancer Ther. 4 (2005) 125–139.
[26] I.R. Hardcastle, C.E. Arris, J. Bentley, F.T. Boyle, Y.H. Chen, N.J. Curtin, J.A. Endicott, A.E. Gibson, B.T. Golding, R.J. Griffin, P. Jewsbury, J. Menyerol, V. Mesguiche, D.R. Newell, M.E.M. Noble, D.J. Pratt, L.Z. Wang, H.J. Whitfield, J. Med. Chem 47 (2004) 3710–3722.
[27] K. Bettayeb, N. Oumata, A. Echalier, Y. Ferandin, J.A. Endicott, H. Galons, L. Meijer, Oncogene 27 (2008) 5797–5807.
[28] P.G. Wyatt, A.J. Woodhead, V. Berdini, J.A. Boulstridge, M.G. Carr, D.M. Cross, D.J. Davis, L.A. Devine, T.R. Early, J. Med. Chem 57 (2008) 4986–4999.
[29] D. Parry, T. Guzi, W. Seghezzi, K. Paruch, R. Doll, A. Nomeir, Y. Wang, M. Oft, P. Kirschmeier, T. Chen, E. Lees, Presented at the AACR Conference, Los Angeles, CA, (2007) Poster 4371.
[30] M.A. Dickson, G.K. Schwartz, Curr. Oncol. 16 (2009) 120–127.
[31] G.I. Shapiro, R. Bannerji, K. Small, S. Black, P. Statkevich, M. Abutarif, J. Moseley, S. Yao, C.H. Takimoto, M.M. Mita, J. Clin. Oncol 26 (2008) 15S.
[32] S. Ortega, I. Prieto, J. Odajima, A. Martín, P. Dubus, R. Sotillo, J.L. Barbero, M. Malumbres, M. Barbacid, Nat. Genet. 35 (2003) 25–31.
[33] M. Barvian, D.H. Boschelli, J. Cossrow, E. Dobrusin, A. Fattaey, A. Fritsch, D. Fry, P. Harvey, P. Keller, M. Garrett, F. La, W. Leopold, D. McNamara, M. Quin, S. Trumpp-Kallmeyer, P. Toogood, Z.P. Wu, E.L. Zhang, J. Med. Chem. 43 (2000) 4606–4616.
[34] P.L. Toogood, Med. Res. Rev. 21 (2001) 487–498.
[35] D.W. Fry, P.J. Harvey, P.R. Keller, W.L. Elliott, M. Meade, E. Trachet, M. Albassam, X.X. Zheng, W.R. Leopold, N.K. Pryer, P.L. Toogood, Mol. Cancer Ther. 3 (2004) 1427–1437.
[36] S.N. VanderWel, P.J. Harvey, D.J. McNamara, J.T. Repine, P.R. Keller, J. Quin, R.J. Booth, W.L. Elliott, E.M. Dobrusin, D.W. Fry, P.L. Toogood, J. Med. Chem. 48 (2005) 2371–2387.
[37] L. Varagnolo, M.P. Stokkel, U. Mazzi, E.K. Pauwels, Nucl. Med. Biol. 27 (2000) 103–112.
[38] K.S. Pentlow, M.C. Graham, R.M. Lambrecht, F. Daghighian, S.L. Bacharach, B. Bendriem, R.D. Finn, K. Jordan, H. Kalaigian, J.S. Karp, W.R. Robeson, S.M. Larson, J. Nucl. Med. 37 (1996) 1557–1562.
[39] S. Vandenberghe, Nucl. Med. Commun. 27 (2006) 237–245.
[40] G.W. Kabalka, R.S. Varma, Tetrahedron 45 (1989) 6601–6621.
[41] K. Wang, S.J. Adelstein, A.I. Kassis, DMSO increases radioiodination yield of radiopharmaceuticals. Appl. Radiat. Isot. 66 (2008) 50–59.
[42] W.C. Eckelman, Nucl. Med. Biol. Int. J. Radiat. Appl. Instrum. Part B 16 (1989) 233–245.
[43] A.A. Wilson, L. Jin, A. Garcia, J.N. DaSilva, S. Houle, Appl. Radiat. Isot. 54 (2001) 203–208.
[44] F. Graf, L. Koehler, T. Kniess, F. Wuest, B. Mosch, J. Pietzsch [article ID 106378]. J. Oncol. (2009) 1–12.
[45] C. Haase, R. Bergmann, F. Fuechtner, A. Hoepping, J. Pietzsch, J. Nucl. Med. 48 (2007) 2063–2071.
[46] M. Berndt, J. Pietzsch, F. Wuest, Nucl. Med. Biol. 34 (2007) 5–15.
[47] D.W. Fry, D.C. Bedford, P.H. Harvey, A. Fritsch, P.R. Keller, Z.P. Wu, E. Dobrusin, W.R. Leopold, A. Fattaey, M.D. Garrett, J. Biol. Chem. 276 (2001) 16617–16623.